

Inhibition of Rac1 Attenuates Radiation-Induced Lung Injury while Sensitizes Lung Tumor to Radiotherapy

Ni An

Changzheng Hospital

Zhenjie Li

Changzheng Hospital

Xiaodi Yan

Changzheng Hospital

Hainan Zhao

Changhai Hospital

Yajie Yang

Second Military Medical University

Ruling Liu

Second Military Medical University

Yanyong Yang

Second Military Medical University

Fu Gao

Second Military Medical University

Bailong Li

Second Military Medical University

Jianming Cai

Second Military Medical University

Hu Liu (✉ gzsassliuhu@163.com)

Second Military Medical University

Hongbin Yuan

Second Military Medical University

Research

Keywords: radiation-induced lung injury, radiation protection, Rac1, Trp53inp1, tumor radiotherapy

Posted Date: August 3rd, 2020

DOI: <https://doi.org/10.21203/rs.3.rs-51213/v1>

License: © ⓘ This work is licensed under a Creative Commons Attribution 4.0 International License.

[Read Full License](#)

Abstract

Backgrounds: There is still little progress in the effective treatment of radiation-induced lung injury (RILI), a key dose-limiting factor for thoracic radiotherapy. Ras-related C3 botulinum toxin substrate1, Rac1, is a small guanosine triphosphatase involved in various mechanisms of radiation-induced damage and is over-expressed/mutated in various tumors. The gain-of-function mutation of Rac1 mediates tumor cells' resistance to radiotherapy. Therefore, inhibiting Rac1 has the potential of protecting normal tissues from radiation-induced injury, and at the same time, sensitizing tumor to radiation therapy, which makes it a promising ideal target for radiation protection. To investigate the protective effects and mechanisms of Rac1 inhibition on RILI, and explore the possible mechanisms that mediate the differential effects of Rac1 inhibition on normal lung tissue and tumor cells.

Methods: ⁶⁰Co radioactive source was used for ionizing radiation (IR). RILI mouse model was constructed. Influence of Rac1 inhibition which was achieved by Rac1-specific inhibitor, NSC23766, on RILI were studied by H & E and Masson staining, and immunohistochemical staining of vimentin, TGF- β and γ -H₂AX. Normal mouse lung epithelial cell line, MLE-12, and mouse lung cancer cell line, LLC, were used to study the effects of Rac1 inhibition on the cellular level. RNA-seq analysis was used for screening differential gene expression caused by Rac1 knockdown. The molecular mechanisms of Rac1 inhibition were studied at the cellular level. Subcutaneous tumor-bearing nude mouse model and orthotopic lung tumor-bearing mouse model were constructed to verify the bidirectional effects of Rac1 inhibition in vivo.

Results: RILI of mouse was alleviated by intraperitoneal injection of NSC23766. Rac1 inhibition/knockdown reduced the radiation-induced damage of MLE-12 while aggravated that of LLC. Rac1 translocated from cytoplasm to nucleus after radiation. Tumor protein p53-inducible nuclear protein 1, Trp53inp1, was down-regulated by Rac1 knockdown. In vivo study further proved the differential effects of Rac1 inhibition. Rac1 was over-expressed and mutated in LLC cells, and the expression level of Trp53inp1 significantly lower, compared with that of MLE-12.

Conclusion: Rac1 inhibition reduced the radiation-induced damage of normal lung epithelial cells, thereby alleviating RILI of mouse. These effects were partially mediated by down-regulating the expression of Trp53inp1. However, Rac1 inhibition significantly increased the sensitivity of LLC to radiation damage and inhibited its growth. The over-expression and mutation of Rac1, and the significant low expression of Trp53inp1 in LLC, may be the fundamental reasons mediating the differential effects of Rac1 inhibition.

Background

Since invented, radiation therapy (RT) has still been the cornerstone of treatments to many malignant tumors. About 40% of tumor patients received RT, either to cure disease, control local tumor or to relieve symptoms¹. The lung is one of the most sensitive tissues to ionizing radiation², thus, radiation-induced lung injury (RILI) stays a key dose-limiting factor of thoracic radiotherapy¹. However, there is still little progress in the safe and effective treatment of RILI, which significantly affects the treatment of patients

with lung cancer, breast cancer, lymphoma or bone marrow transplantation³, etc. Ideally, radioprotectors should not exert protective effects on tumor cells, in other words, do not affect the killing effects of radiation on tumor cells. Therefore, seeking the molecular target that can mediate such a bidirectional effect has become the key to improving tumor radiotherapy. According to previous studies, being involved in oxidative stress⁴⁻⁶, DNA damage^{7,8} and epithelial-mesenchymal transition (EMT)^{9,10}, Rac1 may be an important molecule that mediates radiation damage. Besides, Rac1 is over-expressed or mutated in various tumors¹¹. The gain-of-function mutation of Rac1 can lead to cancer-related phenotype¹² and also mediates tumor cells' resistance to radiotherapy¹³. Therefore, inhibition of Rac1 has the potential of protecting normal tissues from radiation-induced injury, and at the same time, inhibiting tumor growth and sensitizing tumor to radiation therapy, which makes it a promising ideal molecular target for the protection and treatment of RILI caused by clinical radiotherapy.

Materials And Methods

Experimental Animals

Wild-type C57BL/6 and BALB/cJGpt-Foxn1^{nu}/Gpt (nude) male mice at 6~8 weeks of age were purchased from the Experimental Animal Center of Second Military Medical University (SMMU) and GemPharmatech Co, Ltd, respectively. Mice were kept in the animal room of the Department of Radiation Medicine, Faculty of Naval Medicine, SMMU, in a 12h-12h day-night rhythm with plenty of food and water. All animal operating met the requirements of the ethics committee of SMMU.

RILI Mouse Model

C57BL/6 mice were anesthetized and then immobilized in a circumscribed box in which only the lungs of mice were exposed to radiation; the other parts of the box were shielded with lead. Lungs were radiated with a total dose of 25 Gy and a dose rate of 1 Gy/min. The radiation source was ⁶⁰Co from the Radiation Center (Faculty of Naval Medicine, Second Military Medical University).

Subcutaneous Tumor-Bearing of Nude Mice

BALB/cJGpt-Foxn1^{nu}/Gpt mice were subcutaneously injected with 1×10^6 of Rac1-NC/Rac1-SH LLC cells on the right hind leg. Tumor volume (mm³) of each mouse was measured by a Vernier caliper on the 12nd, 15th, 18th, 21st and 24th days after tumor-bearing, and was calculated as the longest diameter (mm)×the shortest diameter (mm)².

Orthotopic Lung Tumor-Bearing Mouse Model

After cell counting, each mouse was injected with 2×10^6 corresponding cells (LLC) suspended in a 50ul mixture of 1:1 medium and matrigel, on the right lung through incision under the right axillary. On the designed week after tumor bearing, mice from each group were sacrificed by cervical dislocation and the tumor mass of each mouse was measured.

Cell Lines

Mouse lung epithelial cell line, MLE-12 (ATCC® CRL-2110™), and mouse lung cancer cell line, LLC (ATCC® CRL-1642™), were cultured in an incubator under a condition of 5% CO₂, 37°C, using DME/F12 1:1 (1×) and DMEM/HIGH GLUCOSE medium, respectively.

Construction of Rac1 Knockdown Cell Lines

Rac1 (Gene ID: 19353) knockdown (SH) and control lentiviral-vectors were purchased from OBiO Technology (Shanghai) Corp., Ltd. A total of 3 targeting-sequences were designed: GGAGACGGAGCTGTTGGTAAA (shRNA1), ATGTCCGTGCAAAGTGGTATC (shRNA2), GCTTGATCTTAGGGATGATAA (shRNA3). MLE-12 and LLC cells were seeded in 12-well plates in a density of 1×10^5 cells/well. 500µl culture medium was added, Rac1-shNC (control) and 3 targets of Rac1-SH were added with a MOI of 20 (for MLE-12) and 10 (for LLC), respectively. Polybrene was added with a final concentration of 1:1000. After 24 hours of virus infection, 500µl culture medium was added and cells were incubated for another 24 hours. Successful virus infection was confirmed by a fluorescence microscope.

Construction of Trp53inp1 Overexpression Cell Lines

Trp53inp1 (Gene ID: 60599) overexpression (OE) and control (NC) lentiviral vectors were purchased from OBiO Technology (Shanghai) Corp., Ltd. Trp53inp1-OE/NC MLE-12 cell lines were constructed on the basis of Rac1-shNC/SH MLE-12 cells, yielding a total of 4 kinds of genetically modified MLE-12 cells, Rac1-shNC∩Trp53inp1-NC (represented as NC-NC), Rac1-SH∩Trp53inp1-NC (SH-NC), Rac1-shNC∩Trp53inp1-OE (NC-OE) and Rac1-SH-Trp53inp1-OE (SH-OE).

Apoptosis and EdU Cell Proliferation Detection

Annexin V-FITC/PI Cell Apoptosis Detection Kit (TransGen Biotech Corp., Ltd, Beijing, China) and Annexin V, 633 Apoptosis Detection Kit (Dojindo Corp., Ltd, Shanghai, China) were used for apoptosis detection of cell lines. BeyoClick™ EdU-594 Cell Proliferation Kit with Alexa Fluor 594 was purchased from Beyotime Biotechnology. Specific operation methods were proceeded according to manufacturer's instructions. Detection was done by flow cytometry.

Western Blotting (WB)

7.5% (PG111) and 12.5% (PG113) PAGE Gel Fast Preparation Kits were purchased from Epizyme Biotech Corp., Ltd, Shanghai, China. Gels were prepared according to manufacturer's instruction. Beta Tubulin Antibody (66240-1-Ig), GAPDH Antibody (60004-1-Ig), BAX Antibody (50599-2-Ig) and BCL2 Antibody (12789-1-AP) were purchased from Proteintech™, Wuhan, China. Anti-Caspase-3 antibody (ab13847), Anti-Cyclin D1 antibody (ab134175), Anti-CDK1 antibody (ab131450), Anti-Cyclin B1 antibody (ab181593), Anti-ATR (phospho T1989) antibody (ab227851), Anti-Chk1 (phospho S345) antibody (ab47318) and Anti-gamma H2A.X (phospho S139) antibody (ab11174) were purchased from Abcam

(Shanghai) Corp., Ltd, China. Anti-Rac1 monoclonal antibody (ARC03) and Anti-Active Rac1-GTP Mouse Monoclonal Antibody (26903) were purchased from Cytoskeleton and NewEast Biosciences, respectively. Anti-rabbit IgG, HRP-linked Antibody (7074) and Anti-mouse IgG, HRP-linked Antibody (7076) were purchased from Cell Signaling Technology (Shanghai) Corp., Ltd, China. Analysis of WB results was done by Image J software.

Co-Immunoprecipitation

Co-immunoprecipitation was conducted strictly in accordance with the manufacturer's instruction provided by Cell Signaling Technology (Shanghai) Corp., Ltd, China. All operations were performed on ice. Samples were boiled in 100°C water bath for 5min and stored in -20°C.

RNA-Seq Analysis

Rac1-shNC and Rac1-SH MLE-12 were seeded in 60mm-dishes at a density of 1×10^6 cells/dish (N=3) and incubated for 24hs. Medium was removed and cells were washed with sterilized PBS and then lysated with 1 ml/dish TRIzol™ Reagent (Thermo Fisher Scientific). Cell lysate was kept frozen with dry ice and sent to Shanghai OE Biotech Corp., Ltd for RNA-Seq analysis.

Statistical Analysis

Statistical analysis was conducted using SPSS19.0 software. Data is expressed as mean±SEM. Student's t test was used for comparing data between two groups. Analysis of Variance (ANOVA) was used when there were multiple groups and SNK-q test was used for further multiple comparison between groups. Difference was considered as statistically significant if $P \leq 0.05$.

Results

1. RILI was Alleviated by Rac1 Inhibition

Compared with the Naive group, the alveolar septum of the IR group at each time points was significantly thickened and the alveolar infiltrated with inflammatory cells (Figure 1A-B), the proportion of collagen fibers increased significantly from the 1st week to the 12th week (Figure 1C-D), indicating that pulmonary inflammation and fibrosis was induced by IR. Intraperitoneal injection of NSC23766, an inhibitor of Rac1¹⁴, could significantly alleviate RILI both in the Low dose (4mg/kg) and the High dose (8mg/kg) groups, manifested as reduction in the thickening of the alveolar septum (Figure 1A-B) and decrease in collagen fiber proportion (Figure 1C-D). Besides, the IR-induced up-regulation of Vimentin, γ -H₂AX and TGF- β , which were important indicators of epithelial-mesenchymal transition (EMT)¹⁵, DNA damage and IR-induced injury, were also inhibited by NSC23766 treatment (Figure 1E-F, Supplemental material, S1A-D). These results supported that inhibition of Rac1 could produce a protective effect on the lung tissue against RILI in mouse model.

2. Radiation-Induced Injury of Mouse Lung Epithelial Cell Line was Alleviated by Rac1 Inhibition/Knockdown

MLE-12 was used for investigation of the effects of Rac1 inhibition in vitro. Cell apoptosis was significantly induced, and the expression of apoptosis-related proteins, Cleaved Caspase-3 and Bax, significantly up-regulated by 10Gy of radiation (Supplemental material, S2B-E). 100 μ M NSC23766 pre-treatment (dose determined by CCK-8 Test in Supplemental material S3A) could reduce the apoptosis ratio (Supplemental material, S3B-C) and decrease the up-regulation of Cleaved Caspase-3 and Bax at 24hs after radiation (Supplemental material, S3D-E).

For further investigating the roles of Rac1 in radiation-induced injury, Rac1 knockdown (Rac1-SH) and control (Rac1-shNC) MLE-12 cell lines were constructed. After verifying the knockdown efficiency by qPCR and WB (Supplemental material, S3), shRNA1 was used for further experiments. 24hs after 10Gy of radiation, the apoptosis ratio and the expression level of Cleaved Caspase-3 of Rac1-SH MLE-12 were significantly lower than those of the control group (Figure 2A-D). Moreover, the expression levels of p-ATR, p-CHK1 and γ -H₂AX, which were all classic indicators of DNA damage response (DDR), were significantly reduced by Rac1 knockdown at 0.5h after 10Gy of radiation (Figure 2E-F). Collectively, our results indicated that radiation-induced injury of MLE-12 were alleviated by Rac1 inhibition/knockdown.

3. Identification of Trp53inp1 as the Critical Downstream Target of Rac1

To further investigate the downstream target of Rac1, RNA-seq analysis was performed. Quality control results proved that the within-group difference of each group was small and the correlation between the two groups was good (supplemental material, S4A-D). Differential genes screening between groups was based on the significant level of $P \leq 0.05$ and fold change of $|\log_2 FC| \geq 0.58$. A total of 262 differential genes were caused by Rac1 knockdown, of which 205 genes were down-regulated and 57 up-regulated (Figure 3A-D). Gene ontology and KEGG pathway analyses showed that these genes are mostly involved in cellular processes of transport and catabolism, and cell growth and death, and are related with human diseases including infectious disease and cancers, and may influence genetic information processes including replication and repair (supplemental material, S4E-G).

According to the molecular biological functions of differential genes and relative literature research, 14 genes of interest were further analyzed by qPCR. Results showed that Rac1 knockdown cell line was successfully constructed (Figure 3E), 8 of 14 genes were significantly down-regulated or up-regulated and changes were consistent with results from RNA-seq analysis (supplemental material, S5B, C, E-I and Figure 3F), 6 of 14 genes were not significantly changed ($P \leq 0.05$) while their trends of up-regulation or down-regulation were consistent with results from RNA-seq analysis (supplemental material, S5A, D, J-M). qPCR results further validated the reliability of RNA-seq. Among these genes, TRP53INP1 was of most interest, which was significantly down-regulated by Rac1 knockdown ($P \leq 0.001$) (Figure 3F).

Human tumor protein p53-induced nuclear protein 1 (*TP53INP1*) is a p53 target gene and encodes the TP53INP1 protein¹⁶ which is mainly expressed in the nucleus¹⁶ and mediates p53-dependent apoptosis

and DNA damage¹⁷. The same gene of mice is named Trp53inp1. According to previous research¹⁶, various cellular stress stimuli including γ -radiation could induce the expression of TP53INP1 which further stimulates the transcriptional activation of p53-target gene promoters. During γ -radiation induced DNA damage, the mRNA level of TP53INP1 in embryonic fibroblasts (MEF) of p53^{+/+} mice was significantly increased, while that of p53^{-/-} mice was not¹⁷, indicating that DNA damage induced TP53INP1 expression is highly dependent on endogenous p53¹⁷.

To investigate whether the protective effects of Rac1 inhibition was mediated by down-regulating Trp53inp1, Trp53inp1 overexpression (OE) and negative control (NC) MLE-12 cell lines were constructed on the basis of Rac1-NC and Rac1-SH MLE-12 cells, yielding a total of 4 kinds of genetically modified MLE-12 cells. The apoptosis ratio of the four groups were similar before IR treatment and were all significantly increased 24hs after 10Gy of radiation (Figure 3G-H). 24hs after 10Gy of radiation, compared with NC-NC group, the apoptosis ratio of NC-OE group was significantly higher ($P < 0.05$), that of the SH-NC group significantly lower ($P < 0.001$) (Figure 3G-H). The apoptosis ratio of SH-OE group was significantly higher than the SH-NC group ($P < 0.001$) but still lower than the NC-NC group (Figure 3G-H). WB assay demonstrated that the expression levels of Cleaved Caspase-3 and Bax in the four groups were increased after IR (Figure 3 I-J). 24hs after IR, compared with the NC-NC group, the expression levels of Cleaved Caspase-3 and Bax in the SH-NC group were significantly lower (both $P \leq 0.001$), however, that of Cleaved Caspase-3 in the NC-OE group significantly higher ($P \leq 0.001$) and that of Bax was of no significant difference (Figure 3 I-J). The expression levels of Cleaved Caspase-3 and Bax in the SH-OE group were significantly higher than those in the SH-NC group (both $P \leq 0.001$).

Consistent with our previous results, the expression levels of p-ATR, p-Chk1 and γ -H₂AX in the SH-NC group were all significantly lower than those of the NC-NC group at 0.5h after radiation (Figure 3K-L). The expression level of p-ATR in the NC-OE group was significantly higher ($P \leq 0.001$), the p-CHK1 significantly lower ($P \leq 0.001$) and the γ -H₂AX of no significant difference than those of the NC-NC group (Figure 3K-L). The expression levels of p-ATR and p-CHK1 in the SH-OE group were significantly higher than those of SH-NC group ($P \leq 0.001$ and 0.05, respectively), the expression level of γ -H₂AX was higher but lack of statistical significance (Figure 3K-L).

Collectively, these results showed that Rac1 knockdown could reduce the apoptosis and DNA damage of MLE-12 after radiation, and Trp53inp1 overexpression could partially reverse this protective effect of Rac1 knockdown.

4. Radiation Induces Nuclear-Translocation of Rac1 and subsequently Prolonged the Residence Time of p53 in the Nucleus

According to previous study¹⁸, when cells faced damage caused by IR, p53 translocated from the cytoplasm into the nucleus and initiated the transcription of Trp53inp1, thereby inducing cell cycle arrest and enhancing p53-mediated apoptosis. Therefore, inhibition of Rac1 may affect the reaction of p53 to radiation stimulation, thereby further down-regulate the expression of Trp53inp1. To verify this

hypothesis, the localization of Rac1 and p53 before and after 10Gy of radiation were investigated by confocal microscopy. Results showed that the translocation of Rac1 and p53 from cytoplasm to nucleus started from 30 minutes, peaked at 2hs and subsided at 6hs after radiation (Figure 4A). Compared with the PBS group, the nuclear-translocation of Rac1 was reduced and subsided earlier (from 2hs after radiation) in the NSC group (treated with 100 μ M NSC23766) (Figure 4A), and the residence time of p53 in the nucleus and its expression level were significantly reduced (Figure 4A). Besides, the cytoplasmic protein and nucleoprotein of MLE-12 were separated before (0h) and after 10Gy of radiation. Results showed that the expression level of Rac1 in the nucleoprotein were increased from 30 minutes and peaked at 2hs after IR (Figure 4B). Further, co-immunoprecipitation analysis showed that Rac1 could bind with p53 (Figure 4C), and inhibition of Rac1 by NSC23766 reduced the up-regulation of p53 induced by IR (Figure 4C). These results showed that radiation could induce the nuclear-translocation of Rac1 and p53, and inhibition of Rac1 could block the nuclear-translocation of Rac1 and reduce the residence time of p53 in the nucleus, indicating that nuclear-translocation of Rac1 could prolong the residence time of p53 in the nucleus, thereby promoting Trp53inp1 transcription.

5. Rac1 knockdown Aggravated the Radiation-Induced Injury of LLC

To date, the main mechanism of action of most radioprotective agents under investigation is to reduce ROS injury. Since oxidative stress injury is one of the main mechanisms of radiation-induced damage, the main problem of these agents is that they also have the potential to protect tumor cells from radiation-induced damage, which is a "side effect" that our investigators do not want. It is important to find a target that can protect normal cells from radiation damage, and in the meantime, do not affect the killing effect of radiation on tumor. Therefore, we further investigated the effects of Rac1 inhibition/knockdown on the radiation-induced injury of mouse lung cancer cells, LLC.

Successful construction of Rac1-SH and Rac1-shNC LLC were verified by WB (supplementary material, S6). 24hs after 10Gy of IR, the apoptosis ratio of Rac1-SH LLC was significantly higher than that of Rac1-shNC LLC ($P \leq 0.001$) (Figure 5A-B) and the expression levels of Cleaved Caspase-3 and Bax significantly higher (both $P \leq 0.01$) (Figure 5C-D). Compared with each of their own basal levels (0h), the expression levels of p-ATR, p-CHK1 and γ -H₂AX were significantly increased from 0.5h after 10Gy of radiation (Figure 5E). The expression levels of p-ATR, p-CHK1 and γ -H₂AX in the Rac1-SH LLC at several time points after IR were significantly higher than those of Rac1-shNC LLC (Figure 5 E). Collectively, our experiments indicated that radiation-induced injury of mouse lung cancer cell line was aggravated by Rac1 knockdown.

6. In Vivo Investigation of the Differential Effects of Rac1 Inhibition/knockdown

First, subcutaneous tumor-bearing nude mice model was constructed with Rac1-NC/SH LLC. The tumor volumes of Rac1-SH group on the 15th and 24th days after tumor-bearing were significantly smaller than those of the Rac1-NC group (N=7, $P \leq 0.05$) (Figure 6 A-B), indicating that the growth of LLC was significantly inhibited by Rac1 knockdown.

Further, orthotopic lung tumor-bearing study was designed. Figure 6C was the illustration of orthotopic lung tumor-bearing and LLR operation. There was no significant difference in tumor mass between the two groups at one week after tumor-bearing ($P=0.568$) (Figure 6D-E). After one week of PBS or NSC23766 (NSC for short) administration in the 2nd week, within the same main group (NC group or SH group), the tumor mass of NSC subgroup was significantly smaller than that of the PBS subgroup (both $P\leq 0.01$) (Figure 6F-G). There was no significant difference between the tumor mass of NC+PBS group and that of SH+PBS group, and there was no significant difference between the tumor mass of NC+NSC group and that of SH+NSC group, either ($P=0.2355$ and 0.2160 , respectively) (Figure 6F-G). Radiation intervention was then proceeded. Three weeks after tumor-bearing that was one week after radiation, among the four non-irradiated groups (no IR): (1) The tumor mass of the NC+NSC group, SH+PBS group and SH+NSC group were all significantly smaller than that of the NC+PBS group ($P\leq 0.05$, 0.01 and 0.001 , respectively) (Figure 6H-I). (2) The tumor mass of the SH+NSC group was significantly than that of NC+NSC group ($P\leq 0.01$) (Figure 6H-I). (3) There was no significant difference between the tumor mass of the SH+NSC group and that of SH+PBS group ($P=0.0515$) (Figure 6H-I). These results showed that tumor growth was significantly inhibited by radiation or NSC23766-induced inhibition of Rac1 alone, tumor growth of Rac1-SH LLC was significantly slower than that of Rac1-NC LLC. Among the four IR groups, only the tumor mass of SH+NSC group was significantly smaller than that of NC+PBS group ($P\leq 0.05$) (Figure 6H-I), suggesting that radiation itself produced a strong inhibitory effect on tumor and that Rac1 knockdown/inhibition alone could not exert a more significant inhibitory effect at this time point, whereas combination of Rac1 knockdown and inhibition could further inhibit tumor growth and show a synergistic effect. No mice from the four no-IR groups survived by the end of the 4th week, which was possibly due to organ failure caused by tumor invasion, thus data were only provided for the four IR groups. The tumor mass of NC+NSC and SH+PBS groups were significantly smaller than that of NC+PBS group (both $P\leq 0.05$) (Figure 6J-K), the difference between those of the SH+NSC group and the NC+PBS group was even more significant ($P\leq 0.01$) (Figure 6J-K). These results showed that the growth of LLC cells was significantly inhibited by Rac1 knockdown and that the combination of Rac1 knockdown and inhibition had a stronger inhibitory effect on tumor growth.

As described above, contralateral non-tumor-bearing lungs were collected for H&E staining on one and two weeks after radiation. Purpose of this part of study was to test whether the radiation-induced injury of contralateral lung could be alleviated by Rac1 inhibition in the same mouse model used for the study of Rac1 knockdown effects on tumor growth. Results showed that: (1) One week after radiation, the thickness of alveolar septum among the four no-IR groups were of no significant difference with one another (Figure 6L-M), and those in the corresponding four IR groups were significantly thickened by radiation treatment (Figure 6L-M). (2) One week after radiation, the thickness of alveolar septum in the NC+NSC group and the SH+NSC group were significantly smaller than those of the NC+PBS group and the SH+PBS group, respectively ($P\leq 0.01$ and $P\leq 0.001$, respectively) (Figure 6L-M), similar results were seen on two weeks after radiation (both $P\leq 0.001$) (Figure 6N-O). These results proved that radiation-induced lung inflammation was alleviated by intraperitoneal injection of Rac1 inhibitor.

7. Possible Mechanisms of the Differential Effects of Rac1 Inhibition/knockdown

Many studies^{11,12} showed that Rac1 was mutated or abnormally activated in tumors, which promoted tumor phenotype and mediated tumor's resistance to various therapies. Consistent with this, Rac1 in LLC cells was significantly over-expressed than that in MLE-12 cells ($P=0.05$) (Figure 7A-B). What's more, exon sequencing analysis showed that there were two insertion segments in the RAC1 gene of LLC (Figure 7C-D). The insertions could contain multiple fragments due to the overlap in the sequencing peaks.

Besides, qPCR and WB results showed that the basal expression level of Trp53inp1 in LLC was significantly lower than that in MLE-12 (both $P=0.001$) (Figure 7E-H). Therefore, due to the extremely low background expression of Trp53inp1, inhibition of Rac1 in LLC cells may not be able to mediate its protective effects of reducing apoptosis and DNA damage by further down-regulating Trp53inp1.

What's more, 10 μ M~100 μ M of NSC23766 treatment did not affect the proliferation ability of MLE-12 (supplemental material, S2A), while same doses of NSC23766 significantly inhibited the proliferation ability of LLC (supplemental material, S7A). Consistent with these, the proliferation ability of LLC both before (0Gy) and 24hs after 10Gy of radiation were significantly inhibited by Rac1 knockdown (Figure 7I-J), however, those of the MLE-12 were not significantly affected (supplemental material, S7B-C). Thus, we further analyzed changes of cell cycle regulatory proteins (cyclins) in LLC. Results showed that the expression levels of Cyclin D1, CDK1 and Cyclin B1 in Rac1-SH LLC were significantly down-regulated compared with those in Rac1-shNC LLC at multiple time points (Figure 7K-N). According to previous research¹⁹, the main function of Cyclin D1 is to promote cell proliferation, in addition, Cyclin D1 is overexpressed in many cancers including lung cancer²⁰ and has been regarded as a proto-oncogene. Cyclin B1 usually begins to be synthesized in the late G1 phase²¹ and reaches a certain level after the cell cycle enters the G2 phase. By binding and activating CDK1, Cyclin B1 promotes the shift from G2 phase to M phase²¹. Also, Cyclin B1 is overexpressed in various cancers including lung cancer²². Thus, there are many differences in the expression of cyclins between tumor cells and normal cells, which also mediates the high proliferation and differentiation ability of tumor cells. Our results showed that Rac1 knockdown could exert a relatively general inhibitory effect on various cyclins of tumor cells, thereby significantly inhibiting the proliferation activity of tumor cells. This proliferation inhibitory effect was not obvious in normal lung epithelial cells.

Discussion

In addition to traditional supportive treatment and anti-inflammatory treatment with steroid¹, a variety of radioprotective agents are being developed. However, there is only one type of radioprotective agent, amifostine, approved for clinical use²³, and the obvious side effects and poor tolerability limit its clinical application^{24,25}. Besides, how to protect normal tissues from radiation damage and at the same time ensure the targeted killing of tumor cells by radiotherapy is an important clinical dilemma. There is still an

urgent need to find such a molecular target. Through the study and summary of previous research²⁶⁻²⁹, Rac1 inhibition was expected to be such a target.

The protective effects of Rac1 inhibition was studied at animal and cellular levels. Results showed that the radiation-induced injury of mouse lung and MLE-12 cells were alleviated by Rac1 inhibition. RNA-seq and qPCR analyses showed that Trp53inp1 was down-regulated by Rac1 knockdown. What's more, the nuclear-translocation of Rac1 and p53 were induced by radiation. Inhibition of Rac1 could block the nuclear-translocation of Rac1 and reduce the residence time of p53 in the nucleus, thereby down-regulating the expression of Trp53inp1 and reducing the apoptosis and DNA damage of MLE-12 after γ -radiation.

Interestingly, unlike MLE-12, Rac1 inhibition/knockdown aggravated the radiation-induced injury of LLC. The reasons by which Rac1 inhibition mediates its differential effects are as followed: First, the Rac1 of normal lung epithelial cells stays normal but is over-expressed and mutated in tumor cells, which may lead to different intracellular biological functions. According to previous studies¹¹⁻¹³, over-activation of Rac1 is associated with tumor phenotype and also mediates tumor tolerance to targeted therapy. Consistent with these, our study showed that Rac1 inhibition sensitized LLC to radiation-induced injury. Secondly, inhibition of Rac1 down-regulated Trp53inp1 in normal cells, the latter mediates p53-specific apoptosis and DNA damage pathway. Noticing that the expression of Trp53inp1 in LLC is significantly lower than that of MLE-12, therefore, it lacks the effects of Rac1 inhibition mediated by down-regulating Trp53inp1 expression, namely reducing p53-related apoptosis and DNA damage. Last but not least, many cyclins are mutated or up-regulated in most tumor cells, which significantly increases their proliferation activity^{20,22}. Our study showed that Rac1 inhibition significantly reduced the expression of various cyclins in and the proliferation activity of LLC. This proliferation inhibitory effect was not obvious in MLE-12.

Finally, the effects of Rac1 inhibition on normal lung tissues and lung tumor were further verified in vivo. Results from nude mice subcutaneous tumor-bearing showed that the tumor volumes were significantly reduced by Rac1 knockdown. Orthotopic lung cancer tumor-bearing study showed that the tumor mass was significantly reduced by Rac1 inhibition/knockdown, meanwhile, the radiation-induced injury of non-tumor-bearing contralateral lungs was significantly alleviated by Rac1 inhibition.

Conclusion

Our study supported that inhibition of Rac1 could not only protect normal lung tissue from radiation-induced injury, but also sensitize lung tumor cells to radiation damage, making it a promising intervention target. The protective effects of Rac1 inhibition was achieved partially by down-regulating Trp53inp1 which is crucially involved in the p53-specific apoptosis and DNA damage signaling pathways. The over-expression and mutation of Rac1 and the extremely low expression of Trp53inp1 in lung tumor cells may be the fundamental reasons for the differential effects of Rac1 inhibition on normal lung tissue and tumor. This is the first study to prove this bidirectional effect of Rac1 inhibition on the animal level, and also the first to discover the interaction of Rac1 with Trp53inp1, indicating a new mechanism for the

complex interaction between Rac1-signalling and p53-signalling. Our results may also provide some new angles for the prevention and treatment of RILI caused by chest radiotherapy.

List Of Abbreviations

Radiation-induced lung injury (RILI), Epithelial-mesenchymal transition (EMT), Radiation therapy (RT), Tumor control probability (TCP), Guanosine triphosphatases (GTPases), Protein p53-induced nuclear protein 1 (TP53INP1), Embryonic fibroblasts (MEF), Overexpression (OE), Negative control (NC), DNA double-strand breaks (DSBs)

Declarations

Ethics approval and consent to participate

All animal experiments were undertaken in accordance with the National Institute of Health "Guide for the Care and Use of Laboratory Animals" (NIH Publication No.85-23, National Academy Press, Washington, DC, revised 1996), with the approval of the Laboratory Animal Center of Second Military Medical University. (approval ID: #201812132).

Consent for publication

All authors reached an agreement to publish the study in this journal.

Availability of data and material

All data generated or analyzed during this study were included in this published article and its supplemental material.

Conflict of interests

The authors have no potential conflict of interests.

Funding

This study was supported in part by the grants from the Pyramid of Talents Project of Shanghai Changzheng Hospital and National Natural Science Foundation of China (No. 81803169 and No. 11635014)

Authors' contributions

Hongbin Yuan, and Hu Liu designed the study. Ni An, Zhenjie Li, Xiaodi Yan, Hainan Zhao, Yajie Yang performed the experiments. Ruling Liu and Yanyong Yang analyzed the data. Ni An and Hu Liu wrote the paper, Hongbin Yuan, Jianming Cai and Hu Liu supported fund assistance. Fu Gao and Bailong Li checked the data. All authors read and approved the final manuscript.

Acknowledgements

We appreciate the radiation device department of Second Military Medical University, which produced gamma-rays.

References

1. Rajan Radha R, Chandrasekharan G. Pulmonary injury associated with radiation therapy - Assessment, complications and therapeutic targets. *Biomed Pharmacother* 2017;89:1092–1104.
2. Giridhar P, Mallick S, Rath GK, Julka PK. Radiation induced lung injury: Prediction, assessment and management. *Asian Pacific J Cancer Prev* 2015;16(7):2613–2617.
3. Jaeger K De, Seppenwoolde Y, Boersma LJ, et al. Pulmonary function following high-dose radiotherapy of non-small-cell lung cancer. *Int J Radiat Oncol Biol Phys* 2003;55(5):1331–1340.
4. Senan S, Ruyscher D De, Giraud P, Mirimanoff R, Budach V. Literature-based recommendations for treatment planning and execution in high-dose radiotherapy for lung cancer. *Radiother Oncol* 2004;71(2):139–146.
5. Borst GR, Ishikawa M, Nijkamp J, et al. Radiation pneumonitis after hypofractionated radiotherapy: evaluation of the LQ(L) model and different dose parameters. *Int J Radiat Oncol Biol Phys* 2010;77(5):1596–1603.
6. Bracci S, Valeriani M, Agolli L, Sanctis V De, Maurizi Enrici R, Osti MF. Renin-Angiotensin System Inhibitors Might Help to Reduce the Development of Symptomatic Radiation Pneumonitis After Stereotactic Body Radiotherapy for Lung Cancer. *Clin Lung Cancer* 2016;17(3):189–197.
7. Bokoch GM, Diebold BA. Current molecular models for NADPH oxidase regulation by Rac GTPase. *Blood* 2002;100(8):2692–2696.
8. Diekmann D, Abo A, Johnston C, Segal AW, Hall A. Interaction of Rac with p67phox and regulation of phagocytic NADPH oxidase activity. *Science* 1994;265(5171):531–533.
9. Price MO, Atkinson SJ, Knaus UG, Dinauer MC. Rac activation induces NADPH oxidase activity in transgenic COSphox cells, and the level of superoxide production is exchange factor-dependent. *J Biol Chem* 2002;277(21):19220–19228.
10. Prakobwong S, Yongvanit P, Hiraku Y, et al. Involvement of MMP-9 in peribiliary fibrosis and cholangiocarcinogenesis via Rac1-dependent DNA damage in a hamster model. *Int J cancer* 2010;127(11):2576–2587.
11. Bopp A, Wartlick F, Henninger C, Kaina B, Fritz G. Rac1 modulates acute and subacute genotoxin-induced hepatic stress responses, fibrosis and liver aging. *Cell Death Dis* 2013;4(3):e558.
12. Santibáñez JF, Kocić J, Fabra A, Cano A, Quintanilla M. Rac1 modulates TGF-beta1-mediated epithelial cell plasticity and MMP9 production in transformed keratinocytes. *FEBS Lett* 2010;584(11):2305–2310.

13. Ungefroren H, Witte D, Lehnert H. The role of small GTPases of the Rho/Rac family in TGF-beta-induced EMT and cell motility in cancer. *Dev Dyn* 2018;247(3):451–461.
14. De P, Aske JC, Dey N. RAC1 Takes the Lead in Solid Tumors. *Cells* 2019;8(5).
15. Watson IR, Li L, Cabeceiras PK, et al. The RAC1 P29S hotspot mutation in melanoma confers resistance to pharmacological inhibition of RAF. *Cancer Res* 2014;74(17):4845–4852.
16. Cardama GA, Alonso DF, Gonzalez N, et al. Relevance of small GTPase Rac1 pathway in drug and radio-resistance mechanisms: Opportunities in cancer therapeutics. *Crit Rev Oncol Hematol* 2018;124:29–36.
17. Jansen S, Gosens R, Wieland T, Schmidt M. Paving the Rho in cancer metastasis: Rho GTPases and beyond. *Pharmacol Ther* 2018;183(September 2017):1–21.
18. Zhang H, Wu X, Xiao Y, et al. Coexpression of FOXC1 and vimentin promotes EMT, migration, and invasion in gastric cancer cells. *J Mol Med (Berl)* 2019;97(2):163–176.
19. Lomax ME, Folkes LK, O'Neill P. Biological consequences of radiation-induced DNA damage: relevance to radiotherapy. *Clin Oncol (R Coll Radiol)* 2013;25(10):578–585.
20. Giuranno L, Ient J, Ruyscher D De, Vooijs MA. Radiation-Induced Lung Injury (RILI). *Front Oncol* 2019;9:877.
21. Cano CE, Gommeaux J, Pietri S, et al. Tumor protein 53-induced nuclear protein 1 is a major mediator of p53 antioxidant function. *Cancer Res* 2009;69(1):219–226.
22. Okamura S, Arakawa H, Tanaka T, et al. p53DINP1, a p53-inducible gene, regulates p53-dependent apoptosis. *Mol Cell* 2001;8(1):85–94.
23. Tomasini R, Seux M, Nowak J, et al. TP53INP1 is a novel p73 target gene that induces cell cycle arrest and cell death by modulating p73 transcriptional activity. *Oncogene* 2005;24(55):8093–8104.
24. Diehl JA, Cheng M, Roussel MF, Sherr CJ. Glycogen synthase kinase-3beta regulates cyclin D1 proteolysis and subcellular localization. *Genes Dev* 1998;12(22):3499–3511.
25. Yang SX, Hewitt SM, Steinberg SM, Liewehr DJ, Swain SM. Expression levels of eIF4E, VEGF, and cyclin D1, and correlation of eIF4E with VEGF and cyclin D1 in multi-tumor tissue microarray. *Oncol Rep* 2007;17(2):281–287.
26. Porter LA, Donoghue DJ. Cyclin B1 and CDK1: nuclear localization and upstream regulators. *Prog Cell Cycle Res* 2003;5:335–347.
27. Ye C, Wang J, Wu P, Li X, Chai Y. Prognostic role of cyclin B1 in solid tumors: a meta-analysis. *Oncotarget* 2017;8(2):2224–2232.
28. Graves PR, Siddiqui F, Anscher MS, Movsas B. Radiation pulmonary toxicity: from mechanisms to management. *Semin Radiat Oncol* 2010;20(3):201–207.
29. Dziegielewska J, Baulch JE, Goetz W, et al. WR-1065, the active metabolite of amifostine, mitigates radiation-induced delayed genomic instability. *Free Radic Biol Med* 2008;45(12):1674–1681.
30. Koukourakis MI. Radiation damage and radioprotectants: new concepts in the era of molecular medicine. *Br J Radiol* 2012;85(1012):313–330.

31. Bourhis J, Blanchard P, Maillard E, et al. Effect of amifostine on survival among patients treated with radiotherapy: a meta-analysis of individual patient data. *J Clin Oncol* 2011;29(18):2590–2597.
32. Kawazu M, Ueno T, Kontani K, et al. Transforming mutations of RAC guanosine triphosphatases in human cancers. *Proc Natl Acad Sci U S A* 2013;110(8):3029–3034.
33. Bright MD, Clarke PA, Workman P, Davies FE. Oncogenic RAC1 and NRAS drive resistance to endoplasmic reticulum stress through MEK/ERK signalling. *Cell Signal* 2018;44:127–137.
34. Hodakoski C, Hopkins BD, Zhang G, et al. Rac-Mediated Macropinocytosis of Extracellular Protein Promotes Glucose Independence in Non-Small Cell Lung Cancer. *Cancers (Basel)* 2019;11(1).
35. Cardama GA, Alonso DF, Gonzalez N, et al. Relevance of small GTPase Rac1 pathway in drug and radio-resistance mechanisms: Opportunities in cancer therapeutics. *Crit Rev Oncol Hematol* [Internet] 2018;124(November 2017):29–36. Available from: <https://doi.org/10.1016/j.critrevonc.2018.01.012>
36. Laufs U, Kilter H, Konkol C, Wassmann S, Böhm M, Nickenig G. Impact of HMG CoA reductase inhibition on small GTPases in the heart. *Cardiovasc Res* 2002;53(4):911–920.
37. Wassmann S, Laufs U, Bäumer AT, et al. Inhibition of geranylgeranylation reduces angiotensin II-mediated free radical production in vascular smooth muscle cells: involvement of angiotensin AT1 receptor expression and Rac1 GTPase. *Mol Pharmacol* 2001;59(3):646–654.
38. Hordijk PL. Regulation of NADPH oxidases: the role of Rac proteins. *Circ Res* 2006;98(4):453–462.

Figures

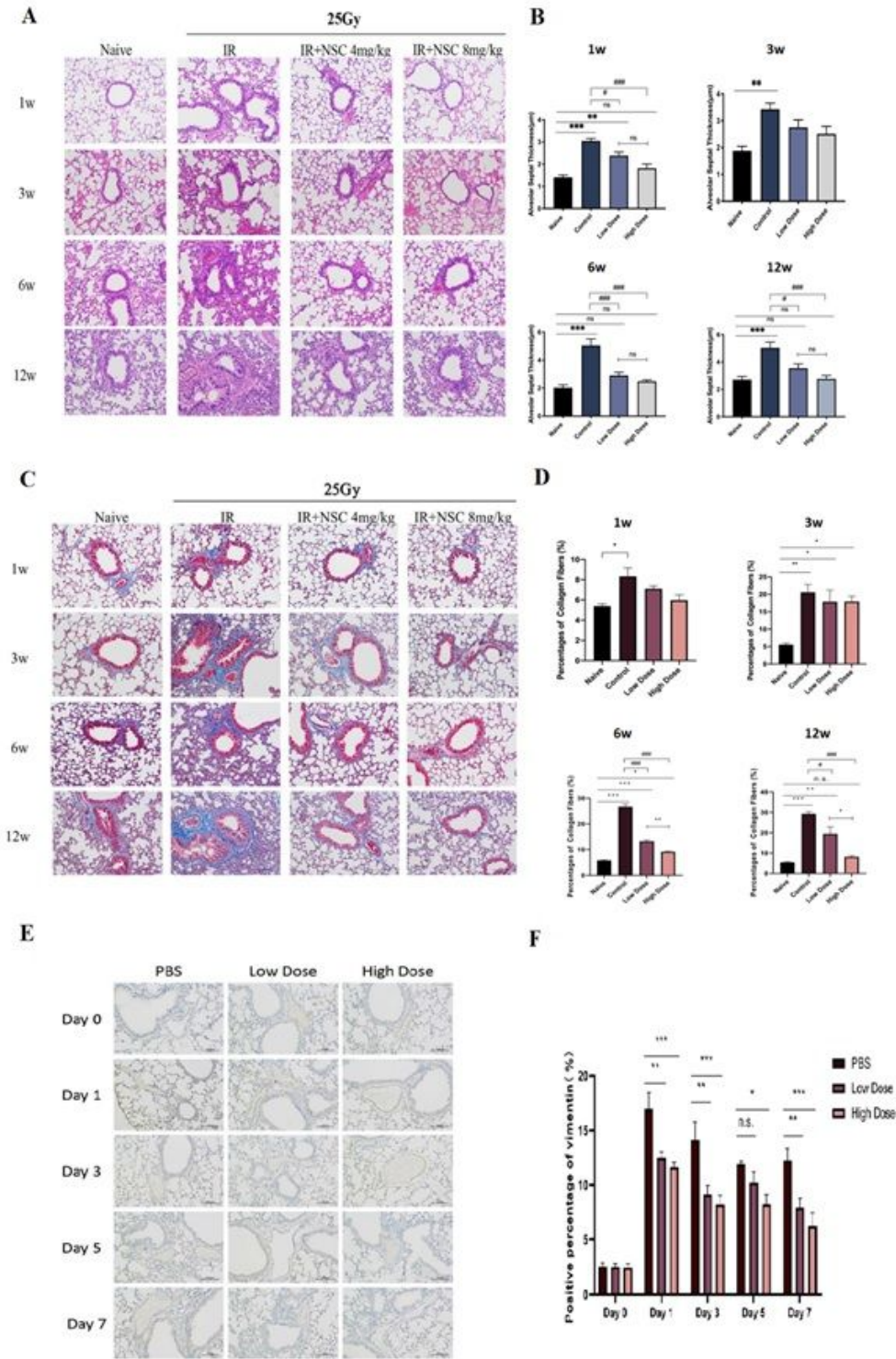


Figure 1

Radiation-induced lung injury was alleviated by Rac1 inhibition. C57BL/6 were randomly divided into four groups which were Naive (no IR+PBS), IR (IR+PBS), Low-Dose (IR+4mg/kg NSC23766) and High-Dose (IR+8mg/kg NSC23766) (N=20). Rac1 inhibition was achieved by intraperitoneal injection of NSC23766, a specific Rac1 inhibitor. Intraperitoneal injection of PBS or NSC23766 was given once a day for a consecutive three days. 2 hours after the 3rd injection, all mice except those of the Naive group were

anesthetized and immobilized in a radiation-specific box for 25Gy of local lung irradiation (IR). On the 1st, 3rd, 6th and 12th week after IR, 5 mice from each group were sacrificed and lung tissues were collected. (A, B) Hematoxylin and eosin (H&E) staining and (C, D) Masson staining were conducted for the evaluation of pulmonary inflammation and fibrosis, respectively. (E, F) C57BL/6 mice were randomly divided into three groups, namely the PBS group (IR+PBS), the Low Dose group (IR+4mg/kg NSC23766) and the High Dose group (IR+8mg/kg NSC23766) (N=15). Before radiation treatment (Day 0) and on the 1st, 3rd, 5th and 7th days after IR, lung tissues from 3 mice of each group were collected for immunohistochemistry analysis of vimentin, an important indicator of pulmonary fibrosis and epithelial-mesenchymal transformation (EMT). Image analysis was conducted using Image J software. ns represented that there was no statistically significant difference between the two groups. *, ** and *** represented P <0.05, 0.01 and 0.001 between the corresponding groups, respectively. #, ## and ### represented P<0.05, 0.01 and 0.001 between the corresponding groups, respectively.

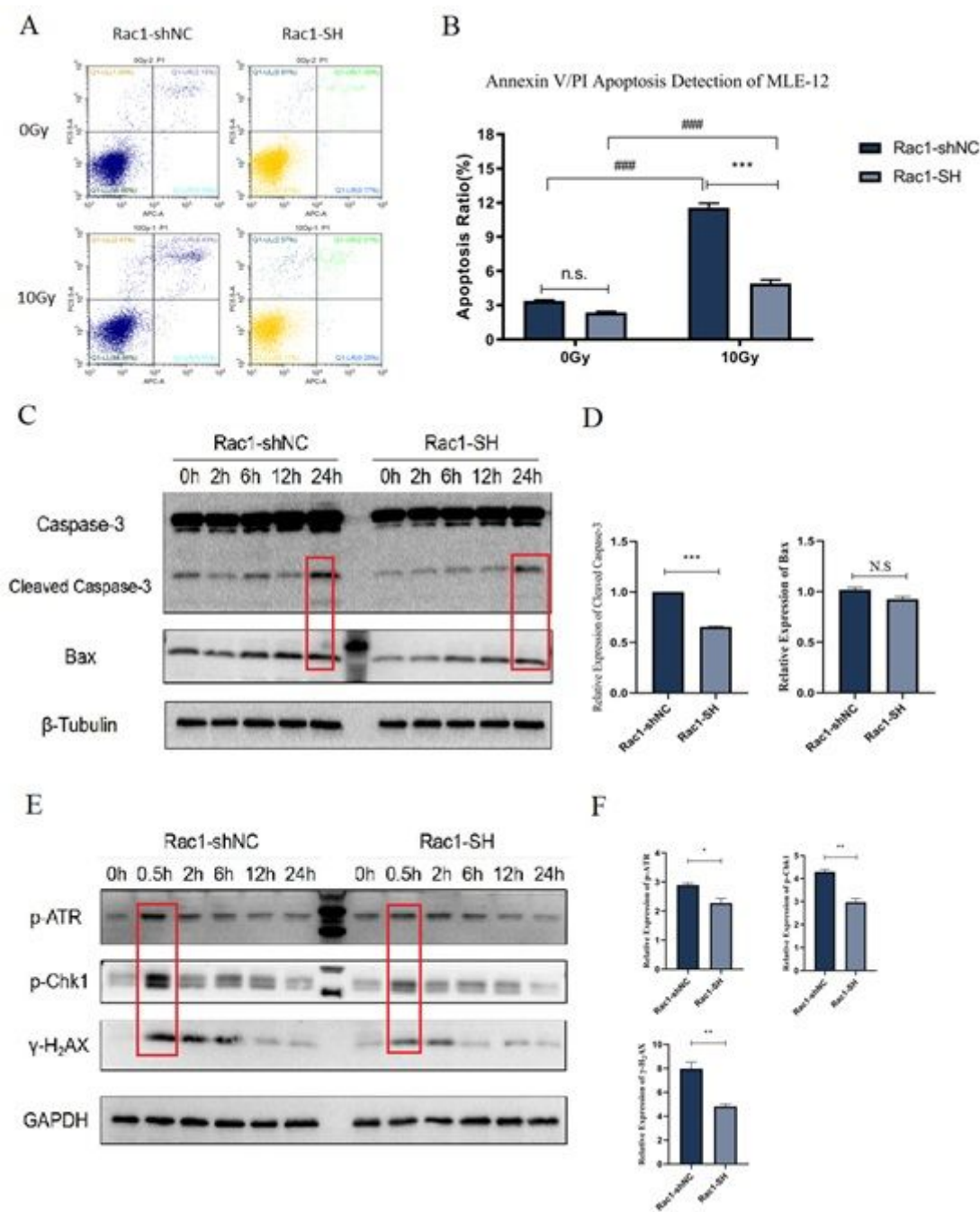


Figure 2

Radiation-induced apoptosis and DNA damage of MLE-12 were reduced by knockdown of Rac1. Rac1 knockdown (Rac1-SH) and control (Rac1-shNC) MLE-12 cell lines were constructed using Lentivirus vector. Cells were collected before (0Gy) and at designed time points after 10Gy of radiation. (A, B) Apoptosis ratio was detected using Annexin V/PI method by a flow cytometer. (C, D) Apoptosis-related proteins, Bax and Caspase-3 were detected by WB analysis. (E, F) Proteins involved in DNA damage response, p-ATR, p-CHK1 and γ -H2AX were detected by WB analysis. ns represented that there was no statistically significant difference between the two groups. *, ** and *** represented $P < 0.05$, 0.01 and 0.001 between the corresponding groups, respectively. ### represented $P < 0.001$ between the corresponding groups. The error value was expressed as mean \pm SEM. N=3 for flow cytometer analysis.

WB analysis was repeated for three times. Identification of Trp53inp1 as the critical downstream target of Rac1 by RNA-Seq analysis. RNA-seq and qPCR analysis of differential expression genes between Rac1-knockdown (Rac1-SH) and control (Rac1-NC) MLE-12. (A) Cluster analysis results of differential expression genes. (B-D) MA diagram, Volcano map and histogram of differential expression genes. Red column represents the genes up-regulated by Rac1-knockdown, and blue represents the genes down-regulated. $P < 0.05$, $|\log_2FC| > 0.58$. A total of 262 differential genes were caused by Rac1 knockdown, of which 205 genes were down-regulated and 57 genes were up-regulated. (E and F) qPCR analysis of relative gene expression level of Rac1 and Trp53inp1 between Rac1-SH and Rac1-NC MLE-12. Trp53inp1 over-expression (OE) and negative control (NC) MLE-12 cell lines were constructed on the basis of Rac1-NC and Rac1-SH MLE-12 cells, yielding a total of 4 kinds of genetically modified MLE-12 cells, which were Rac1-NC-Trp53inp1-NC (represented as NC-NC), Rac1-SH-Trp53inp1-NC (represented as SH-NC), Rac1-NC-Trp53inp1-OE (represented as NC-OE) and Rac1-SH-Trp53inp1-OE (represented as SH-OE). All 4 kinds of cells were collected before (0Gy) and at designed time points after 10Gy of irradiation. (G, H) Apoptosis ratio detected by a flow cytometer. (I, J) Apoptosis-related proteins, Bax and Caspase-3 were detected by WB analysis. (K, L) Proteins involved in DNA damage response, p-ATR, p-CHK1 and γ -H2AX were detected by WB analysis. ** and *** represented $P < 0.01$ and 0.001 between the corresponding groups, respectively. The error value was expressed as mean \pm SEM. Experiments were repeated for three times.

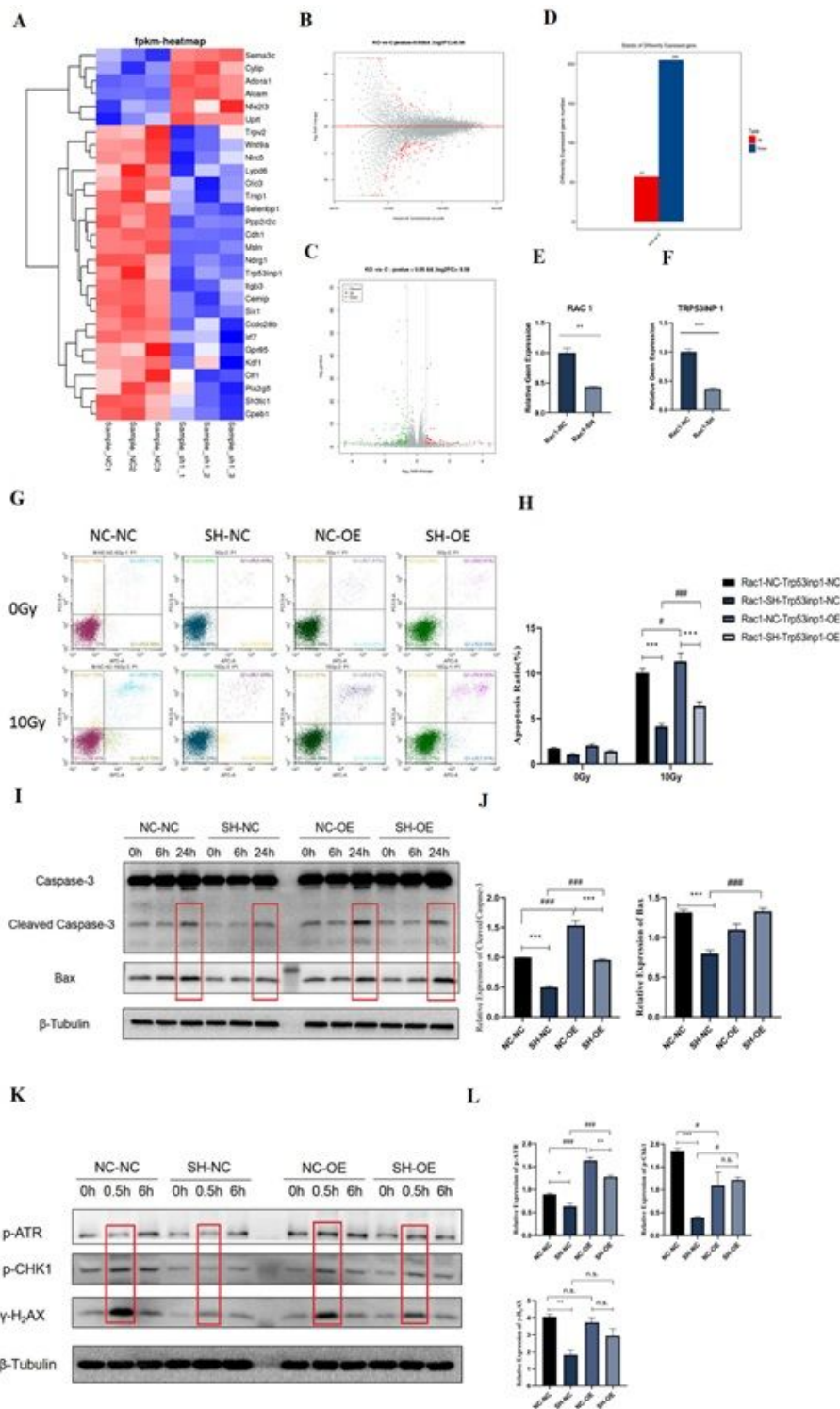


Figure 3

Identification of Trp53inp1 as the critical downstream target of Rac1 by RNA-Seq analysis. RNA-seq and qPCR analysis of differential expression genes between Rac1-knockdown (Rac1-SH) and control (Rac1-NC) MLE-12. (A) Cluster analysis results of differential expression genes. (B-D) MA diagram, Volcano map and histogram of differential expression genes. Red column represents the genes up-regulated by Rac1-knockdown, and blue represents the genes down-regulated. $P \leq 0.05$, $\geq 2FC \geq 0.58$. A total of 262

differential genes were caused by Rac1 knockdown, of which 205 genes were down-regulated and 57 genes were up-regulated. (E and F) qPCR analysis of relative gene expression level of Rac1 and Trp53inp1 between Rac1-SH and Rac1-NC MLE-12. Trp53inp1 over-expression (OE) and negative control (NC) MLE-12 cell lines were constructed on the basis of Rac1-NC and Rac1-SH MLE-12 cells, yielding a total of 4 kinds of genetically modified MLE-12 cells, which were Rac1-NC-Trp53inp1-NC (represented as NC-NC), Rac1-SH-Trp53inp1-NC (represented as SH-NC), Rac1-NC-Trp53inp1-OE (represented as NC-OE) and Rac1-SH-Trp53inp1-OE (represented as SH-OE). All 4 kinds of cells were collected before (0Gy) and at designed time points after 10Gy of irradiation. (G, H) Apoptosis ratio detected by a flow cytometer. (I, J) Apoptosis-related proteins, Bax and Caspase-3 were detected by WB analysis. (K, L) Proteins involved in DNA damage response, p-ATR, p-CHK1 and γ -H2AX were detected by WB analysis. ** and *** represented $P < 0.01$ and 0.001 between the corresponding groups, respectively. The error value was expressed as $\text{mean} \pm \text{SEM}$. Experiments were repeated for three times.

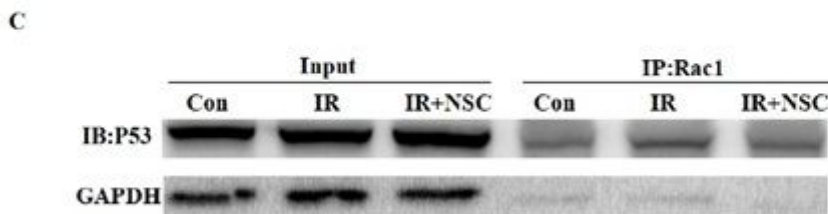
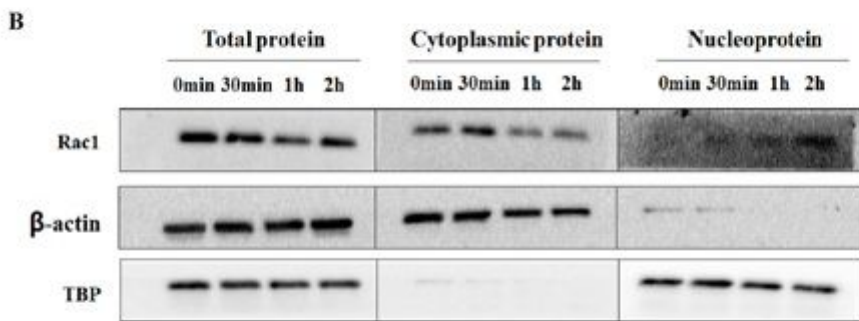
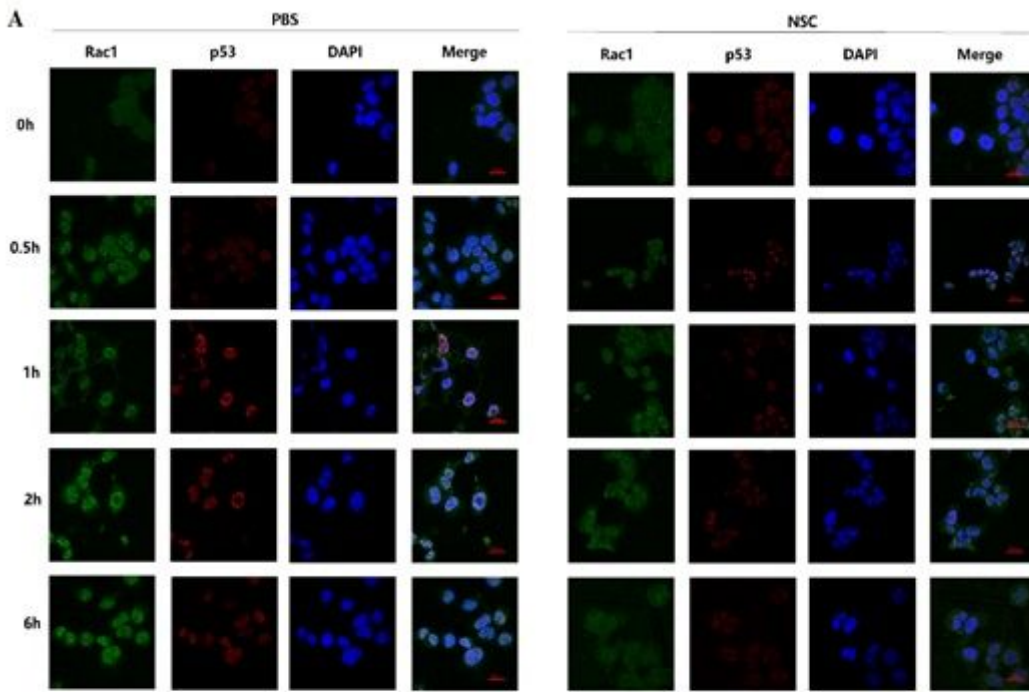


Figure 4

Nuclear translocation of Rac1 was induced by radiation and subsequently prolonged the residence time of p53 in the nucleus by binding with it. MLE-12 cells were pretreated with PBS or NSC23766 (NSC, 100 μ M) for 2hs and then went through 10Gy of radiation. (A) Cells were collected from 0~6hs after radiation for immunofluorescence analysis of the trans-location of Rac1 and p53. Green and Red fluorescence represented Rac1 and p53, respectively. (B) At 0~2hrs after radiation, nucleoprotein and cytoplasmic protein were separated for detection of the subcellular distribution of Rac1 and p53. (C) At 2hs after radiation, immunoprecipitation was conducted to detect the binding of Rac1 with p53.

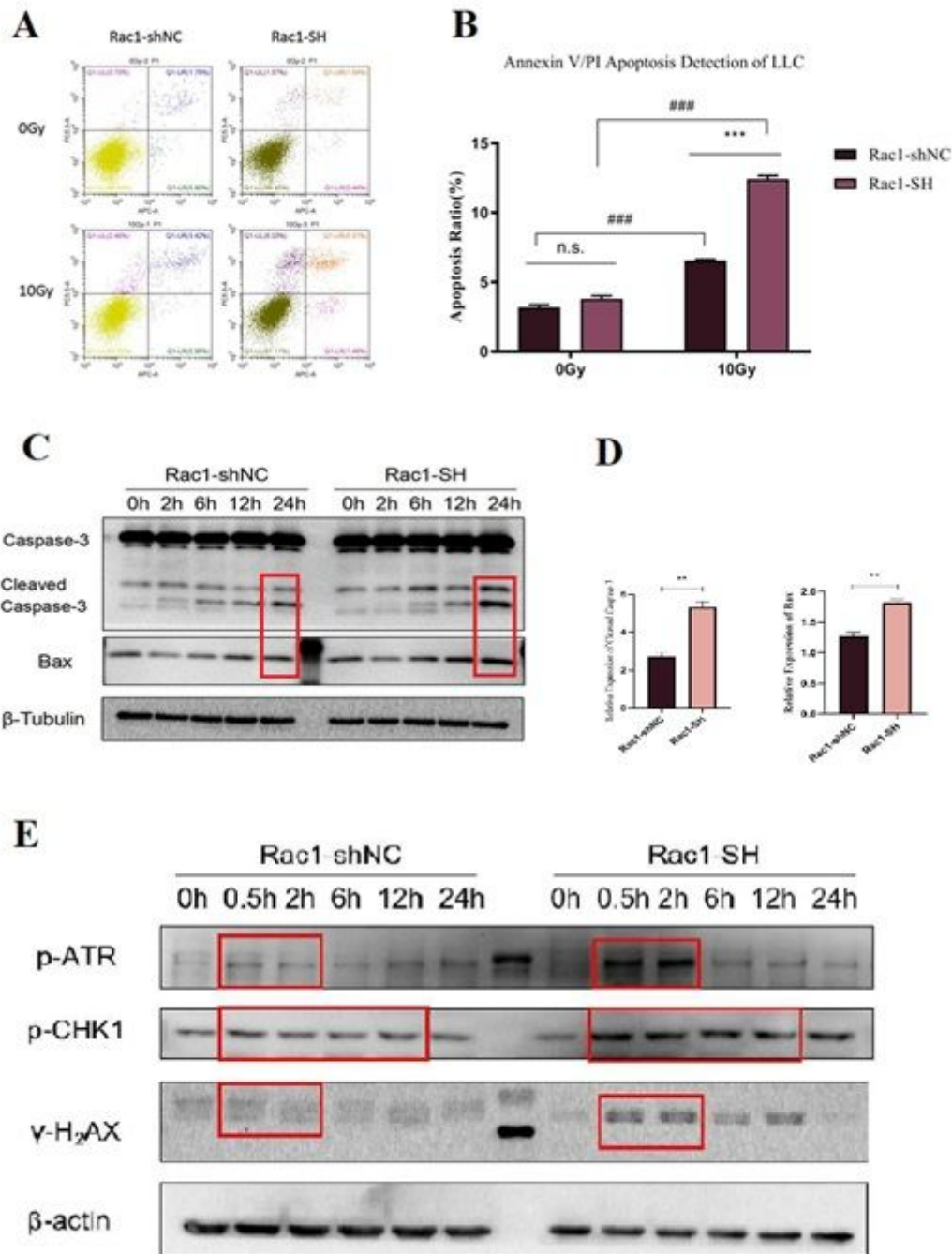


Figure 5

Radiation-induced injury of mouse lung cancer cells, LLC, was aggravated by Rac1 knockdown. Rac1 knockdown (Rac1-SH) and control (Rac1-shNC) LLC cell lines were constructed using Lentivirus vector. Cells were collected before (0Gy) and at designed time points after 10Gy of irradiation. (A, B) Apoptosis ratio detected by Annexin V/PI method through flow cytometer. (C, D) Apoptosis-related proteins, Caspase3 and Bax were detected by WB analysis. (E) Proteins involved in DNA damage response, p-ATR, p-Chk1 and γ -H2AX were detected by WB analysis. ns represented that there was no statistically significant difference between the two groups. *** and ### represented $P < 0.001$ between the

corresponding groups. The error value was expressed as mean±SEM. N=3 for flow cytometer analysis. WB analysis was repeated for three times.

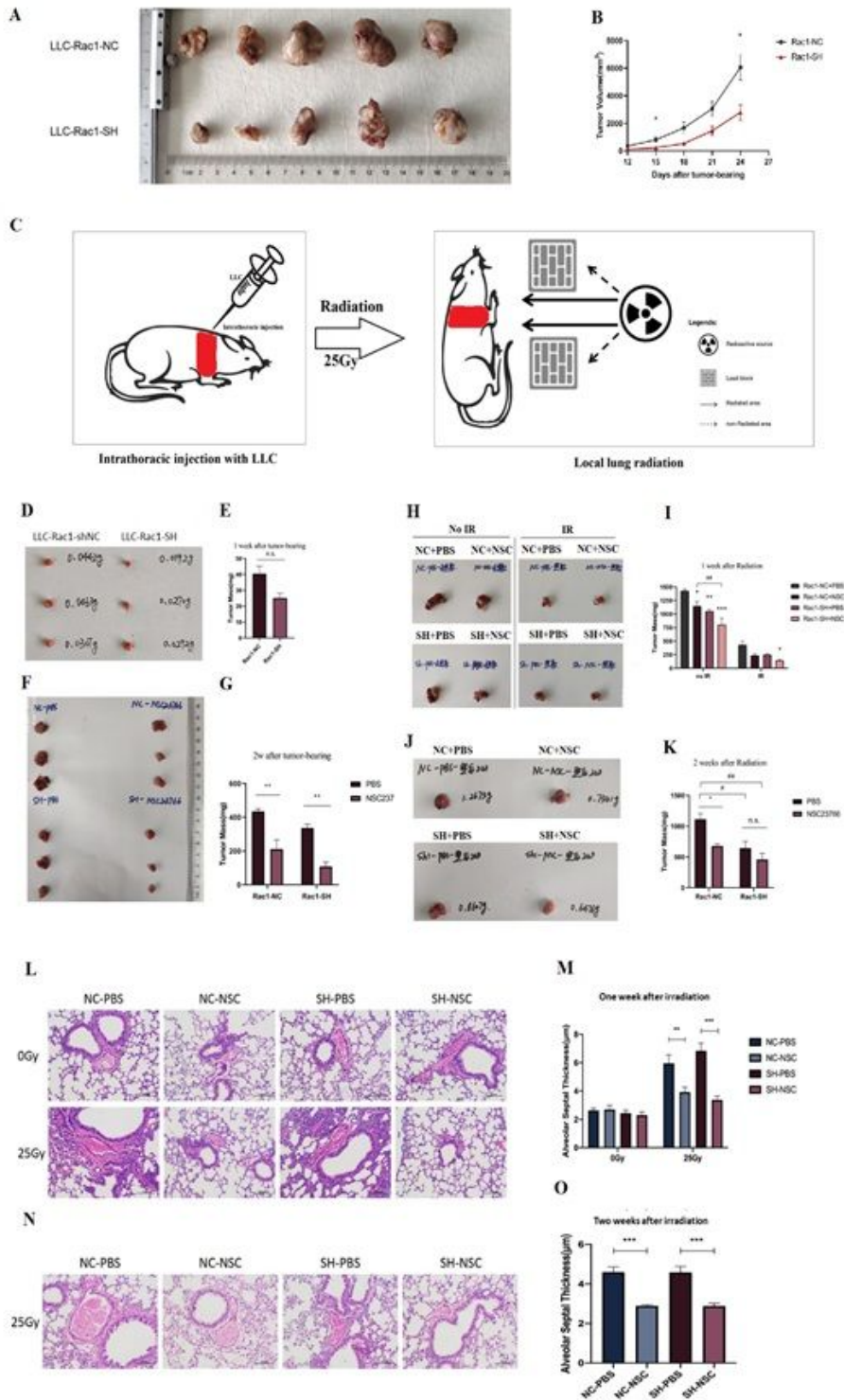


Figure 6

In vivo verification of the differential effects of Rac1 inhibition/knockdown, inhibiting lung tumor while protecting normal lung tissue. (A, B) BALB/cJGpt-Foxn1nu/Gpt mice were randomly divided into two groups, namely the control group (LLC-Rac1-NC) and the Rac1 knockdown group (LLC-Rac1-SH). After ear

labeling, mice were subcutaneously injected with 1×10^6 of corresponding LLC cells on the right hind leg. The control group were injected with Rac1-NC LLC and the Rac1 knockdown group with Rac1-SH LLC. The size of each mouse's tumor was measured with a vernier caliper on the 12nd, 15th, 18th, 21st and 24th days after tumor-bearing. Tumor volume (mm^3) was calculated as the longest diameter (mm) \times the shortest diameter (mm) 2 . (C) Schematic diagram of orthotopic lung tumor-bearing and local lung radiotherapy. (D-K) Orthotopic lung tumor-bearing mouse model. Specific study design was written in detail in the part of Materials and Methods. The tumor volumes of Rac1 knockdown group on the 15th and 24th days after tumor-bearing were significantly smaller than those of the control group ($P \leq 0.05$). (L-O) H & E staining of non-tumor-bearing contralateral lung tissues. NC-PBS, NC-NSC, SH-PBS and SH-NSC represented tumor-bearing with Rac1-NC or Rac1-SH LLCs combined with intraperitoneal injection of PBS or NSC23766 (3mg/kg, on alternate days for a week). (M and O) were the statistical analysis of the thickness of each group's alveolar septum thickness on one and two weeks after local lung irradiation. ** and *** represented $P < 0.01$ and 0.001 between the corresponding groups, respectively. The error value was expressed as $\text{mean} \pm \text{SEM}$. $N=3$.

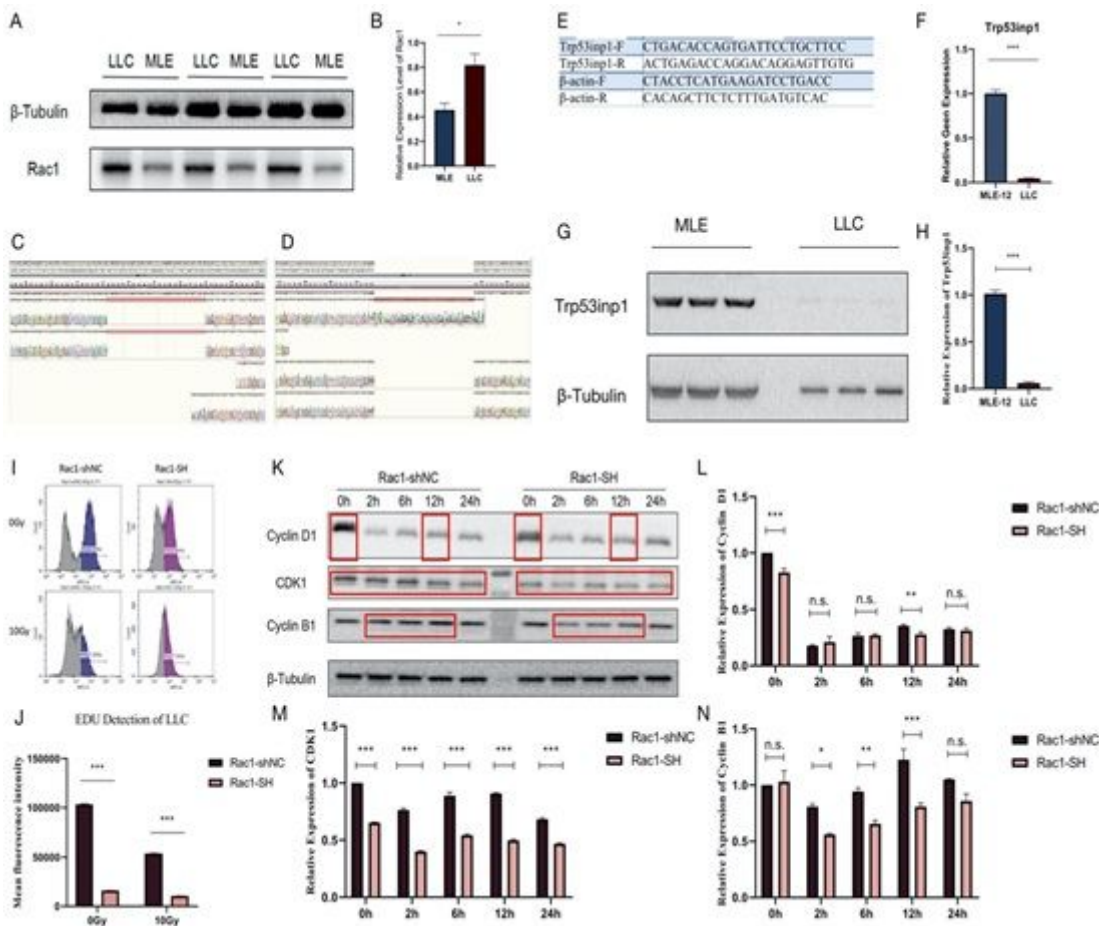


Figure 7

The Over-expression and mutation of Rac1 and the extremely low expression of Trp53inp1 in lung cancer cells may contribute to the differential effects of Rac1 inhibition on normal lung tissue and tumor. (A) WB analysis of the Rac1 expression level in MLE-12 and LLC. (B) was the statistical analysis of the relative gray values of (A). (C and D) Exon sequencing of Rac1 in MLE-12 and LLC. Results showed that there

were two insertion segments in the RAC1 gene of LLC, compared with that of MLE-12. (E and F) qPCR analysis of the Trp53inp1 expression level in MLE-12 and LLC. (E) showed the sequence of primer used. (F) was the relative mRNA level of Trp53inp1. (G and H) WB analysis of the Trp53inp1 expression level in MLE-12 and LLC. (H) was the statistical analysis of the relative gray values of (G). (I and J) EdU detection of Rac1-shNC and Rac1-SH LLC cells by flow cytometer. Cells were collected before (0Gy) and 24hs after 10Gy of irradiation. (J) was the statistical analysis of each group's mean fluorescence intensity. (K-N) WB analysis of cell cycle regulatory proteins. Rac1-shNC and Rac1-SH LLC cells were collected before (0h) and 2~24hs after 10Gy of irradiation. (L), (M) and (N) were the statistical analysis of the relative gray values of Cyclin D1, CDK1, and Cyclin B1 at each time points. ns represented that there was no statistically significant difference between the two groups. *, ** and *** represented $P < 0.05$, 0.01 and 0.001 between the corresponding groups, respectively. Experiment was repeated for three times.

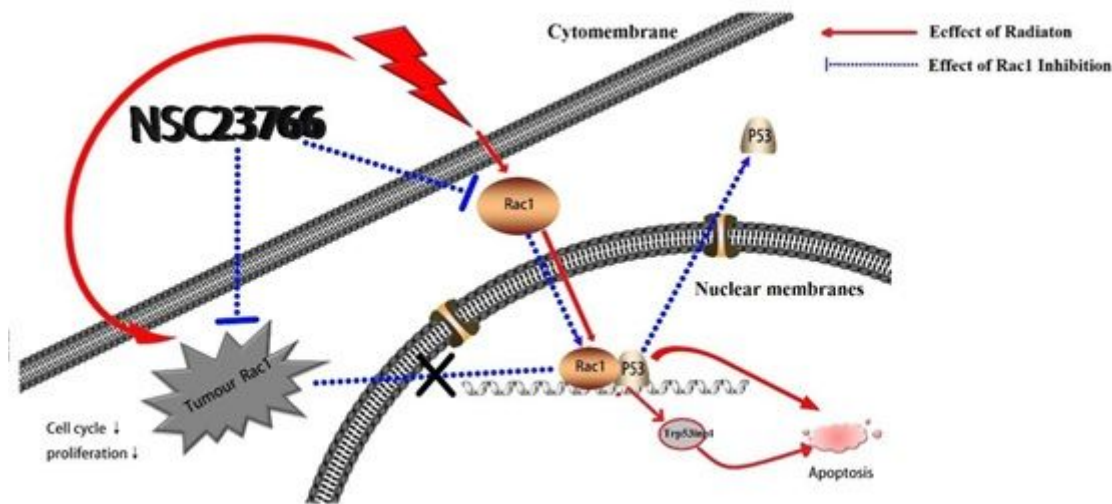


Figure 8

Summary of study. Ionizing radiation induces the nuclear-translocation of Rac1, the latter then binds with p53 and prolongs the residence time of p53 in the nucleus, thereby promoting the transcription of Trp53inp1 which mediates p53-dependent apoptosis. Inhibition of Rac1 with NSC23766 could reduce the nuclear-translocation of Rac1 induced by irradiation, thereby fasting the release of p53 from the nucleus, at last reducing the apoptosis. However, due to the over-expression and mutation of Rac1, and the extremely low expression of Trp53inp1 in tumor cells, inhibition of Rac1 does not reduce the apoptosis of tumor cells after radiation but can inhibit the proliferation ability of tumor cells.

Supplementary Files

This is a list of supplementary files associated with this preprint. Click to download.

- [Supplementalmaterial.docx](#)
- [Supplementalmaterial.docx](#)